DOI: 10.48011/asba.v2i1.1563

Discrete-time $\mathscr{L}_2$ loop-shaping control of a Maglev System using the LPV framework

Luiz Benicio Degli Esposte Rosa * **Renan Lima Pereira** *

* *Instituto Tecnológico de Aeronáutica, Praça Marechal Eduardo Gomes, Vila das Acácias, 12228-900 São José dos Campos, SP, Brazil*
E-mails: engbenicio@gmail.com, renanrlp@ita.br

Abstract: This paper presents a practical application of discrete-time $\mathscr{L}_2$ loop-shaping control to a Maglev system using the linear parameter-varying (LPV) framework. LMI-based conditions are obtained for the synthesis of an output-feedback LPV controller that guarantees robust stability and performance to the closed-loop system. Guidelines to design such controller are given in a simple and transparent manner. In addition, detailed modeling of the didactic plant manufactured by Quanser® is carried out and the process of embedding the nonlinear equations into a discretized quasi-LPV (qLPV) model is described. Simulations and experimental results show that the proposed procedure can be an advantageous alternative to handle nonlinear systems in comparison to its linear time-invariant (LTI) version.

Keywords: Discrete-time LPV systems; $\mathscr{L}_2$ loop-shaping control; Magnetic levitation system; LMIs

1. INTRODUCTION

Magnetic levitation is the core concept in two fields of application: Maglev transportation systems and active magnetic bearings (AMBs). It allows the construction of contactless and frictionless devices, which are highly efficient, reliable, flexible and sustainable, dispensing with lubrication, repairment, and bearing changes (Tonoli et al., 2012). The dynamics of these systems are open-loop unstable, multivariable and nonlinear, requiring sophisticated control systems to operate. Numerous contributions have been made on both areas, using a wide range of control techniques. In particular, parameter-dependent controllers have proved a nice tool to control AMBs, as in Lu et al. (2008) and Balini et al. (2012). They adjust to the rapidly varying operating conditions without the slowly-varying parameters requirement of simpler gain-scheduling techniques. Still, they are yet to be explored for Maglev systems, perhaps due the high gains commonly obtained in continuous-time syntheses, which are not appropriate for implementation. To the best of the authors' knowledge, McCloy et al. (2018) is the only published work to explore LPV controllers for Maglev systems. The authors designed a discrete-time, estimate-based state-feedback, but this technique can be quite cryptic to tune from the designer's point of view . In the present paper, we opt for a robust output-feedback loop-shaping synthesis using the LPV paradigm. The method relies on simple and established notions of control, resulting in straightforward tuning and implementation. In addition, it provides better robustness margins to the closed-loop system.

LPV systems were introduced by Shamma (1988) to provide a framework to the design of inherently gain-scheduled controllers. The idea is to design a parameter-dependent controller that automatically adjusts to plant variation, described in terms of exogenous scheduling parameters available in real time. In a second effort, Shamma and Athans (1990) extended this notion to nonlinear systems, by hiding nonlinearities as varying parameters. This contribution greatly increased the method's potential, since the majority of gain-scheduling applications feature endogenous signals as scheduling parameters. Besides, it enabled the utilization of powerful linear tools for analysis and control design of the class of nonlinear systems known today as qLPV.

In the following years, LPV systems received a lot of attention due to the emergence of powerful computational tools such as linear matrix inequalities (LMIs). Shahruz et al. (1992) investigated the extension of stability with frozen parameters to that of the global system; Balas and Apkarian (1992) introduced qLPV systems with a linear fractional dependence on the scheduling parameters. Becker et al. (1993) dealt with LPV controllers recovering the notion of quadratic stability in Barmish (1985), using inequalities; Packard (1994) tackled discrete-time LPV systems; Becker and Packard (1994) obtained conditions for induced $\mathcal{L}_2$-norm performance for parameter-dependent systems; Apkarian et al. (1995) first used systems with an affine dependence on the varying parameters, now commonly known as polytopic systems. Since then, a vast number of theoretical and practical works regarding LPV systems have been published. Efforts have been made, for example, to reduce conservatism employing parameter-dependent Lyapunov (PDL) functions (Wu, 1995) (Gahinet et al., 1996) (Wang and Balakrishnan, 2002), improve LPV modeling and identification techniques Lovera et al. (2011), extend its application to particular classes of nonlinear systems (Lescher et al., 2006), and obtain conditions for established LTI synthesis procedures in the LPV framework.

⋆

The synthesis used in this work consists of an LPV version of the famed $\mathcal{H}_\infty$ loop-shaping design methodology from McFarlane et al. (1990). Now widely popular, the method combines intuition from classical tools with robustness stabilization and guaranteed performance from $\mathcal{H}_\infty$ optimization. Hence, the designer can easily tune and implement controllers with a transparent trade-off between performance and robust stability objectives. This seminal work has triggered a number of contributions which further improved the method and expanded its scope of applicability. Whidborne et al. (1994) developed a new approach via LMIs; Apkarian and Gahinet (1995) extended its application to LPV systems and LTI systems subject to parametric uncertainty; Gu et al. (2002) obtained LMI conditions for discrete-time LTI systems; Prempain (2004) developed the static approach via LMIs; Pereira et al. (2017b) derived the conditions for a discrete-time version, which was then extended to LPV systems in Pereira et al. (2017a).

Building on these approaches, the $\mathscr{L}_2$ loop-shaping controller proposed here is formulated using the observer-based controller structure in Sefton and Glover (1990) for LPV systems. In this sense, the objective of this paper is to evaluate the practical application of a discrete-time LPV controller to a Maglev system. The LPV controller synthesis is given from LMI conditions, which ensure closed-loop robust stability and performance. The nonlinear plant is described in terms of a discrete-time qLPV model, featuring some state variables as scheduling parameters. It is shown that, by choosing a proportional-integral (PI) compensator as a pre-filter to shape the open-loop model, the $\mathscr{L}_2$ optimization is able to provide a fine response. Finally, the effectiveness of the proposed design is assessed in a Maglev system manufactured by Quanser.

This paper is organized as follows. Section 2 offers some preliminaries definitions; Section 3 describes the synthesis procedure, consisting of two steps: loop shaping design and $\mathscr{L}_2$ optimization. In Section 4, the dynamical equations of the Maglev System are developed and embedded into a discrete-time qLPV model. Section 5 presents the design procedure and results, with a brief comparison to the LTI synthesis. Section 6 contains the conclusions.

The notation used is standard. $\mathbb{R}^{n\times m}$ denotes the set of real $n \times m$ matrices; I is an identity matrix and A^T represents the transpose of a matrix. For square matrices, $det(A)$ is the determinant and $Tr(A)$ the trace of A. If $A = A^T$, $A \succ 0$ ($A \succeq 0$) means that A is positive (semi-)definite and $A \prec 0$ ($A \preceq 0$) that it is negative (semi-)definite. Symmetric blocks in matrices are occasionally indicated by $\star$ and $\|\bullet\|_{i,2}$ stands for the induced-$\mathscr{L}_2$ norm. The notation $G \triangleq \left[\begin{array}{c|c} A & B \\ \hline C & D \end{array}\right]$ is used to represent a state-space realization. $Co(\xi_1, \xi_2, ..., \xi_r)$ is a convex hull with vertices ξ_i. For a concise notation, the dependence of the signals on k will be dropped whenever it is clear.

2. PRELIMINARIES

Discrete-time LPV systems can be represented in state-space as

$$x(k+1) = A(\rho(k))x(k) + B(\rho(k))u(k) \quad (1)$$
$$y(k) = C(\rho(k))x(k) + D(\rho(k))u(k) \quad (2)$$

where $x(k) \in \mathbb{R}^n$ denotes the state vector; $y(k) \in \mathbb{R}^{n_y}$ the vector of measurement outputs and $u(k) \in \mathbb{R}^{n_u}$ the control inputs. A, B, C, D are real-valued rational functions of the time-varying parameter vector $\rho(k) = [\rho_1(k), ..., \rho_m(k)]^T \in \mathbb{R}^m$, which are available in real-time and belong to the unit simplex

$$\Psi = \left\{ \alpha \in \mathbb{R}_+^N : \sum_{i=1}^{N} \alpha_i(k) = 1,\ i = 1, \ldots, N \right\}. \quad (3)$$

The state-space representation for a generalized plant is given by

$$\left[\begin{array}{c} x(k+1) \\ \hline z(k) \\ y(k) \end{array}\right] = \left[\begin{array}{c|c|c} A(\rho) & B_1(\rho) & B_2 \\ \hline C_1(\rho) & D_{11}(\rho) & D_{12}(\rho) \\ C_2 & D_{21}(\rho) & D_{22} \end{array}\right] \left[\begin{array}{c} x(k) \\ \hline w(k) \\ u(k) \end{array}\right]. \quad (4)$$

where $z(k) \in \mathbb{R}^{n_z}$ represents a vector with outputs of interest and $w(k) \in \mathbb{R}^{n_w}$ the exogenous inputs. In this paper, the state-space matrices are assumed to be affine in $\Psi \triangleq Co(\xi_1, \xi_2, ..., \xi_r)$. In addition, only $A(\rho(k))$ is considered to be dependent on the varying parameters, whereas B_2 and C_2 are fixed and D_{22} is null. This can be always achieved with loop transformation and addition of filters (Prempain and Postlethwaite, 2008).

Moreover, some definitions for discrete-time LPV systems regarding performance criteria will be used throughout this paper. Typically, such criteria are used for closed-loop systems. Herein, the closed-loop system T_{zw} adopting a control law given by $u(k) = -K(\rho)y(k)$ in (4) will be addressed.

Definition 1. Suppose that the closed-loop system T_{zw} is exponentially stable. Then its $\mathscr{H}_2$ norm is defined by

$$\|T_{zw}\|_2^2 := \lim_{T\to\infty} E\left\{ \frac{1}{T} \sum_{k=0}^{T} z^T(k) z(k) \right\} \quad (5)$$

when ω_k is a stationary, zero-mean, white noise process with identity covariance matrix.

Definition 2. Suppose that the closed-loop system T_{zw} is exponentially stable. Then its induced $\mathscr{L}_2$ norm is defined by

$$\|T_{zw}\|_{i,2} = \sup_{\|w\|_2 \neq 0} \frac{\|z\|_2}{\|w\|_2} \quad (6)$$

where $z \in \ell_2$ and $w \in \ell_2$ for all $\rho \in \Psi$.

3. $\mathscr{L}_2$ LOOP-SHAPING SYNTHESIS FOR LPV SYSTEMS

3.1 Loop-Shaping Concept

The methodology consists of two steps. First, the open-loop plant is shaped with the addition of pre- and post-compensators in order to achieve desirable closed-loop performance. In this step, classical control rules of thumb can be used to select the filters. Usually, high gains are desirable in lower frequencies to achieve good reference tracking and disturbance rejection, while low gains are preferable in higher frequencies to attenuate noise. At this point, the nominal model $G(\rho)$ is replaced with the shaped model given by

$$G_S(\rho) = W_2(\rho)G(\rho)W_1(\rho). \tag{7}$$

Still, the shaped plant is not necessarily stable once the loop is closed, because this property cannot be inferred from the open-loop system. Thus, the second step is to solve a robust stabilization problem, which ensures closed-loop stability.

3.2 Robust Stabilization Problem

Consider the following representation of the shaped plant

$$G_S(\rho) = [\tilde{M}(\rho) + \Delta_{\tilde{M}}]^{-1}[\tilde{N}(\rho) + \Delta_{\tilde{N}}]. \tag{8}$$

$\tilde{M}(\rho)$ and $\tilde{N}(\rho)$ are left-coprime factors of the plant and $\Delta_{\tilde{M}}$ and $\Delta_{\tilde{N}}$ are stable and unknown mappings of the uncertainties associated to them, defined as

$$\Delta = [\Delta_{\tilde{N}}, \Delta_{\tilde{M}}], \quad \|\Delta\|_{i,2} \leq \epsilon. \tag{9}$$

The robust stabilization problem consists in finding the maximum value of ϵ for which all of the models can be stabilized by the controller $K(\rho)$. Figure 1 shows the topology of the problem.

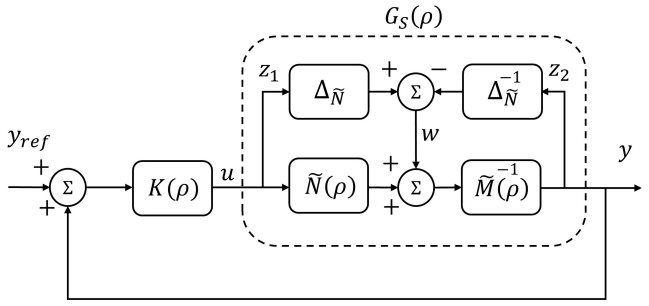

Figure 1. Coprime factor robust stabilization problem.

Taking into account the exogenous outputs $z(k)$ with relation to exogenous inputs $w(k)$, we have

$$z_1 = K(\rho)[I - G(\rho)K(\rho)]^{-1}\tilde{M}^{-1}(\rho)w \tag{10}$$

$$z_2 = [I - G(\rho)K(\rho)]^{-1}\tilde{M}^{-1}(\rho)w. \tag{11}$$

Therefore, the robust stabilization problem can be stated as an optimization problem, as follows

Definition 3. Let$(\tilde{N}(\rho), \tilde{M}(\rho))$ be a contractive left-coprime factorization of $G(\rho)$. Then, the robustness specification, ϵ, such that $G_\Delta(\rho) = (\tilde{M}(\rho) + \Delta_{\tilde{M}})^{-1}(\tilde{M}(\rho) + \Delta_{\tilde{N}})$ can be stabilized by a single controller, $K(\rho)$, for all Δ is given by

$$\left(\inf_{K(\rho)} \left\| \begin{bmatrix} K(\rho) \\ I \end{bmatrix} (I - G(\rho)K(\rho))^{-1}\tilde{M}(\rho)^{-1} \right\|_{i,2} \right)^{-1} < \epsilon \tag{12}$$

where $K(\rho)$ is chosen over all stabilizing controllers.

If the left-coprime factors are normalized, ϵ can be interpreted as an upper bound on the nonparametric uncertainties, i.e., the maximum allowable perturbation to the left-coprime factors of the shaped plant. Conversely, $\gamma = \epsilon^{-1}$ is an upper bound on the induced-$\mathscr{L}_2$ norm from w to z. For LPV systems, normalized coprime factors are very hard if not impossible to obtain, and are not even guaranteed to exist (Beck and Doyle, 1993). The solution lies in the concept of contractiveness (Li and Paganini, 2005), which allows a relaxation of the Riccati equations that ensures stability on the factorization while preserving the convexity of the overall problem. Despite inserting a certain degree of conservatism onto the problem, it provides nice flexibility to accommodate structure constraints and enables the solution via LMIs (Li, 2014).

3.3 LMI-based Solutions

The first step to solve the robust stabilization problem is to find a stabilizing observer gain to construct contractive and parameter-dependent left-coprime factorizations. Prempain (2006) showed that, for continuous-time systems, this gain can be obtained by solving the $\mathscr{H}_2$ filtering problem applied to the output injection open-loop interconnection. This notion was extended to discrete-time systems in the theorem that follows.

Theorem 4. If the pair $(C, A(\rho))$ is detectable in a quadratic sense, then, for any given $\mu > 0$, there is a contractive left-coprime factorization

$$\left[\, \tilde{M}(\rho) \;\; \tilde{N}(\rho) \,\right] \triangleq \left[\begin{array}{c|cc} A(\rho) + HC & H & B \\ \hline Z_2C & Z_2 & 0 \end{array}\right] \tag{13}$$

with $H = P^{-1}Y$ and $Z_2 = (I + CPC^T)^{-1/2}$ if there exist a symmetric matrix $P \in \mathbb{R}^{n\times n}$ and matrices $Y \in \mathbb{R}^{n\times n_y}$ and $X \in \mathbb{R}^{n\times n}$ that satisfy the following optimization problem:

$$\mu^2 = \min trace\,(X) \;, \tag{14a}$$

$$\begin{pmatrix} X & I \\ \star & P \end{pmatrix} \succ 0 \;, \tag{14b}$$

$$\begin{pmatrix} P & PA_i + YC & Y & PB \\ \star & P & 0 & 0 \\ \star & \star & I & 0 \\ \star & \star & \star & I \end{pmatrix} \succ 0 \;, \tag{14c}$$

for $i = 1, ..., N$. The $\mathscr{H}_2$ norm can be calculated from $\mu < \sqrt{trace\,(X)}$.

Proof. The proof is straightforward using the same procedure presented in (Pereira et al., 2017a) for robust case.

After this step, the generalized plant is given by (15) (Gu et al., 2013), which corresponds to the full information structure for LPV systems.

$$G_z(\rho) \triangleq \left[\begin{array}{c|c|c} A(\rho) & -H & B \\ \hline 0 & 0 & I \\ Z_2C & Z_2 & 0 \\ \hline C & I & 0 \end{array}\right]. \tag{15}$$

Next, a state-feedback problem should be solved to satisfy the performance criteria in (12). The LMI-based conditions are given by the following theorem .

Theorem 5. Consider the system (15). There exists a robust state-feedback gain $F = ZW^{-1}$ such that the closed-loop system is stable and the induced-$\mathscr{L}_2$ norm is minimized if there exist $W = W^T \succ 0 \in \mathbb{R}^{n\times n}$ and $Z = Z^T \in \mathbb{R}^{n_u\times n}$ that satisfy the following optimization problem:

$$\min \gamma^2$$
$$\begin{pmatrix} W & AW+BZ & 0 & 0 & -H \\ WA^T+Z^TB^T & W & Z^T & WC^TZ_2^T & 0 \\ 0 & Z & I & 0 & 0 \\ 0 & Z_2CW & 0 & I & Z_2 \\ -H^T & 0 & 0 & Z_2 & \gamma^2 I \end{pmatrix} \succ 0 \tag{16}$$

Proof. Consider the feedback control law $u(k) = Fx(k)$ for the generalized plant (15). Then, after applying the Bounded Real Lemma for discrete-time LPV systems, as presented in (Apkarian et al., 1995), and some mathematical manipulations to avoid nonlinear terms, we obtain condition (16). Hence, the proof is complete.

3.4 Controller Construction

In the previous section, a state-feedback controller is designed for a left-coprime factorization of the shaped plant. The output-feedback loop-shaping controller is given by (Prempain and Postlethwaite, 2008) as an observer-based controller structure,

$$K(\rho) \triangleq \left[\begin{array}{c|c} A(\rho)+BF+HC & H \\ \hline -F & 0 \end{array}\right] \tag{17}$$

However, it depends on ρ and thus can only be computed in real time. From Apkarian and Gahinet (1995), the controller is given by

$$K(\rho) \triangleq \sum_{i=1}^{r} \alpha_i K_i = \sum_{i=1}^{r} \alpha_i \left(\begin{bmatrix} A_{Ki} & B_{Ki} \\ C_{Ki} & D_{Ki} \end{bmatrix} \right) \tag{18}$$

where $\alpha_1, ..., \alpha_r$ is a solution of the convex decomposition problem and K_i represent the vertex controllers

$$\rho = \sum_{i=1}^{r} \alpha_i \xi_i \tag{19}$$

such that ξ_i can be defined as in the following example. Let us examine a system with two varying parameters constrained to lie in a polytope with four vertices

$$\xi_1 \triangleq [\rho_{1_{min}} \quad \rho_{2_{min}}], \quad \xi_2 \triangleq [\rho_{1_{max}} \quad \rho_{2_{min}}], \tag{20}$$
$$\xi_3 \triangleq [\rho_{1_{max}} \quad \rho_{2_{max}}], \quad \xi_4 \triangleq [\rho_{1_{min}} \quad \rho_{2_{max}}]. \tag{21}$$

Then, we have

$$\alpha_1 = \xi_1\xi_2, \quad \alpha_2 = (1-\xi_1)\xi_2, \tag{22}$$
$$\alpha_3 = \xi_1(1-\xi_2), \quad \alpha_4 = (1-\xi_1)(1-\xi_2), \tag{23}$$

where

$$\xi_1 = \frac{\rho_{1_{max}} - \rho_1(k)}{\rho_{1_{max}} - \rho_{1_{min}}}, \quad \xi_2 = \frac{\rho_{2_{max}} - \rho_2(k)}{\rho_{2_{max}} - \rho_{2_{min}}}. \tag{24}$$

Notice that α_i satisfy $0 \leq \alpha_i \leq 1$ and $\sum_{i=1}^{4} \alpha_i = 1$. Hence, they are convex. Such characteristic is given by vertex properties. Now, all that is required is the combination of this controller and the shaping functions to construct the final controller

$$K_F(\rho) = W_1(\rho)K(\rho)W_2(\rho). \tag{25}$$

3.5 Design procedure

Finally, a design control procedure to obtain the $\mathscr{L}_2$ loop shaping controller with guaranteed robustness properties can be summarized as follows:

(1) Initially, select the pre- and post-filters W_1 and W_2 to model the shaped plant $G_S(\rho)$ as in (7).
(2) Determine the observer gain H that composes the left-coprime factorization (13) using Theorem 4.
(3) Determine the robust state-feedback gain F from Theorem 5 to obtain the $\mathscr{L}_2$ controller $K(\rho)$ described in (17) as an observer-based controller structure.
(4) Finally, the feedback controller for implementation $K_F(\rho)$ is given by

$$\begin{bmatrix} x(k+1) \\ x_{w_1}(k+1) \\ \hline x_{w_2}(k+1) \\ \hline u(k) \end{bmatrix} = K_F(\rho) \begin{bmatrix} x(k) \\ x_{w_1}(k) \\ \hline x_{w_2}(k) \\ \hline y(k) \end{bmatrix} \tag{26}$$

such that

$$K_F(\rho) = \left[\begin{array}{ccc|c} A_K(\rho) & 0 & B_K C_{w_2} & B_K D_{w_2} \\ B_{w_1} C_K & A_{w_1} & B_{w_1} D_K C_{w_2} & B_{w_1} D_K D_{w_2} \\ 0 & 0 & A_{w_2} & B_{w_2} \\ \hline D_{w_1} C_K & C_{w_1} & D_{w_1} D_K C_{w_2} & D_{w_1} D_K D_{w_2} \end{array}\right] \tag{27}$$

where the pre- and pos-compensators are described as

$$W_1 = \left[\begin{array}{c|c} A_{w_1} & B_{w_1} \\ \hline C_{w_1} & D_{w_1} \end{array}\right], W_2 = \left[\begin{array}{c|c} A_{w_2} & B_{w_2} \\ \hline C_{w_2} & D_{w_2} \end{array}\right], \tag{28}$$

respectively.

4. LPV MODELING FOR THE MAGLEV SYSTEM

4.1 Dynamical Model Description

The system features a steel ball that should levitate due to the electromagnetic force generated by an electromagnet. The objective is to manipulate the voltage applied to the electromagnet coil in order to control the ball vertical position. Measurements of ball position and coil current are provided by a photosensitive sensor and a resistor, respectively. Figure 2 shows a schematic of the system taken from Quanser's workbook.

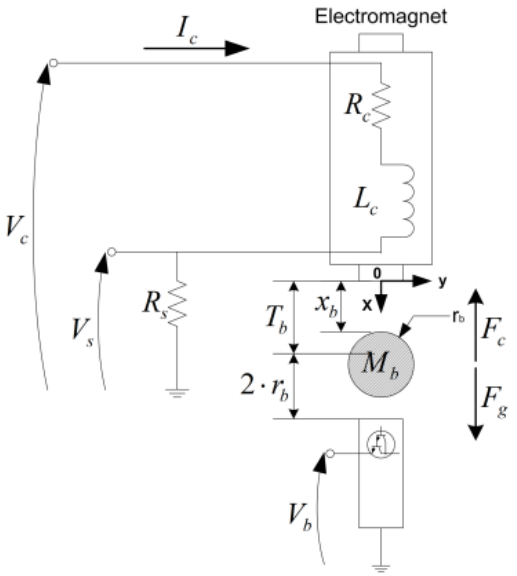

Figure 2. Didactic plant scheme (Quanser, Inc., 2012)

The coil current can be computed using Ohm's and Faraday's laws

$$v_S(t) = R_S i_C(t), \tag{29}$$

where $i_C(t)$ is the current, R_S is the resistance, and $v_S(t)$ is the voltage sense at the current sensing resistor. Faraday's and Kirchoff's laws can then be applied to yield

$$v_C(t) = (R_C + R_S)i_C(t) + \frac{d\Phi(t)}{dt} \tag{30}$$

where $v_C(t)$ is the voltage applied to the coil, R_C is the resistance, and $\Phi(t)$ is the magnetic flux linkage at the coil.

Following the guidelines in (McCloy et al., 2018), the inductance dependence on the ball position is modeled as

$$L(x_b(t)) = L_C + \frac{L_b a}{a + x_b(t)} \tag{31}$$

where L_C is the coil inductance alone, L_b is the ball inductance, and a is a positive constant obtained with experiments. The magnetic flux can be expressed as

$$\Phi(t) = L(x_b(t)) \cdot i_C(t), \tag{32}$$

so the differential equation relating coil current and inductance is

$$\frac{di_C(t)}{dt} = \frac{d}{dt}\frac{\Phi(t)}{L(x_b(t))}. \tag{33}$$

The next step is to equate the forces acting on the ball.

$$F = F_g + F_v + F_C \tag{34}$$

where F_g is the gravity force, F_v is the drag force, and F_C is the force generated by the electromagnet. F_g can be readily obtained as

$$F_g = M_b g \tag{35}$$

where M_b is the ball mass and g is the standard gravity. F_v can be modeled via Stokes law as

$$F_v = -b_v \dot{x}_b(t) \tag{36}$$

where $b_v = 6\pi r_b \mu_v$, r_b is the ball radius and μ_v is magnetic permeability constant. The attractive force exerted by the electromagnet on the ball can be characterized in terms of coenergy

$$F_C = \frac{\partial W_L(i_C(t), L(x_b(t)))}{\partial x_b(t)}. \tag{37}$$

Since the coenergy is given by

$$W_L(i_C(t), L(x_b(t))) = \frac{1}{2}\Big(L_C + \frac{L_b a}{a + x_b(t)}\Big) i_C^2(t), \tag{38}$$

the force can be expressed as

$$F_C = -\frac{L_b a}{2(a + x_b(t))^2} i_C^2(t). \tag{39}$$

At last, Newton's second law gives the equation of motion for the ball

$$M_b \ddot{x}_b(t) = M_b g - b_v \dot{x}_b(t) - \frac{L_b a}{2(a + x_b(t))^2} i_C^2(t) \tag{40}$$

The total inductance will be considered as constant, since the effect of the ball is insignificant in this case. So, a state-space representation of the system is given by

$$\dot{x}_1(t) = \dot{x}_b(t) \tag{41}$$

$$\dot{x}_2(t) = g - \frac{b_v}{M_b} x_2(t) - \frac{L_b a}{2M_b (x_1(t))^2} x_3^2(t) \tag{42}$$

$$\dot{x}_3(t) = \frac{1}{L_C}[u(t) - (R_C + R_S)x_3(t)]. \tag{43}$$

where $x_1(t) = a + x_b(t)$, $x_2(t) = \dot{x}_b$, $x_3(t) = i_C(t)$, and $u(t) = v_C(t)$. System parameters of the didactic plant are given in Table 1 The limitations imposed by physical constraints on states and input excursions are given by

$$10.1\ mm \leq x_1(t) \leq\ 24.1\ mm \tag{44}$$

$$0\ A \leq x_3(t) \leq\ 3\ A \tag{45}$$

$$0\ V \leq\ u(t) \leq\ 24\ V \tag{46}$$

More technical details about the didactic plant manufactured by Quanser® can be viewed in (Quanser, Inc., 2012).

4.2 LPV Model

The objective of using an LPV model is to approximate or even match the mapping of the nonlinear model in a framework where several linear tools are still applicable. In this work, a linearization-based approach is used to obtain an LPV model (Packard, 1994; Toth, 2010). The idea is to obtain Taylor approximations of state and output evolution at a number of equilibrium points. Then, this set of LTI systems can be described as polynomials in terms of the scheduling parameters. The equilibrium points are given by

$$\bar{x}_2 = 0 \tag{47}$$

$$\bar{x}_3 = \sqrt{\frac{2M_b g}{L_b a}}\bar{x}_1 \tag{48}$$

$$\bar{u} = (R_C + R_S)\bar{x}_3. \tag{49}$$

The varying parameters are chosen as $\rho_1(t) = x_1(t)$ and $\rho_2(t) = x_3(t)$, as both states are available in real time. This means the model is qLPV, since the parameters are endogenous signals. To avoid complications due to hard nonlinearities, x_b was restricted to lie between 6 mm and 12 mm, which in turn imposes a restriction on i_C excursion as well. Then, we define the compact set for the varying parameters to be

$$-3\ mm \leq \rho_1(t) \leq\ 3\ mm \tag{50}$$

$$-387\ mA \leq \rho_2(t) \leq\ 387\ mA \tag{51}$$

To synthesize the $\mathscr{L}_2$ controller, the model must be discretized. Exact discretization of LPV systems can be problematic, as the traditional zero-order hold method can inflict loss of convexity, which is key for most controller analysis and synthesis available. Though not exact, forward Euler method is widely employed in the discretization of such systems, since convexity properties are preserved (Apkarian, 1997; Toth, 2010). For a given sampling time T, the discrete-time LPV model is given by

$$x(k+1) = \begin{bmatrix} 1 & T & 0 \\ T\lambda(\rho) & 1 - \dfrac{Tb_v}{M_b} & T\beta(\rho) \\ 0 & 0 & 1 - \dfrac{TR}{L_C} \end{bmatrix} x(k) + \begin{bmatrix} 0 \\ 0 \\ \dfrac{T}{L_C} \end{bmatrix} u(k) \tag{52}$$

Table 1. Maglev system parameters.(Quanser, Inc., 2012)

Parameter	Value
M_b	68 g
μ_v	$4\pi \cdot 10^{-7}$ H/m
r_b	12.7 mm
a	10.1 mm
R_C	10 Ω
R_S	1 Ω
L_C	412.5 mH
L_b	31.7 mH

where $R = R_C + R_S$ and the parameters

$$\lambda(\rho) = 1027.14 - 5.48 \times 10^4 \rho_1 + 4.48 \times 10^4 \rho_1 \rho_2$$
$$\beta(\rho) = -15.91 + 849.49\rho_1 - 693.61\rho_1\rho_2 \quad (53)$$

Notice that if the parameters are restricted to be $\rho(k) = 0$, we get an LTI model at $\bar{x}_b = 9\ mm$ and $\bar{u} = 13.5625\ V$.

5. DESIGN AND RESULTS

5.1 $\mathscr{L}_2$ Controller Design

The goal is to control the steel ball position with zero steady-state error and mininum integral absolute error (IAE), to get a fine trade-off between maximum overshoot and settling time. In addition, robustness specification dictates that the value of γ should be kept below 4.

The first step in the design procedure is to shape the open-loop plant to achieve desired performance. For $T = 2\ ms$, the following pre- and post-compensators were able to provide acceptable performance in the simulation level. Therefore, they were chosen for implementation.

$$W_1(z) = \frac{20.2z - 19.8}{z - 1} \quad (54)$$
$$W_2(z) = 3000. \quad (55)$$

Notice that $W_1(z)$ is a PI compensator, designed in continuous-time for intuitive tuning purposes and discretized via Tustin method.

Then, the $\mathscr{H}_2$ optimization problem was solved. Applying Theorem 4, matrices P and Y were found to be

$$P = \begin{bmatrix} 3.77 & 636.01 & 22.34 & -41.93 \\ \star & 4.09 \cdot 10^7 & -2.30 \cdot 10^5 & -1.82 \cdot 10^4 \\ \star & \star & 2.27 \cdot 10^3 & -85.40 \\ \star & \star & \star & 500.52 \end{bmatrix}, \quad (56)$$

$$Y = \begin{bmatrix} -5.74 \cdot 10^{-4} \\ -2.84 \cdot 10^3 \\ 4.37 \\ 0.11 \end{bmatrix}, \quad (57)$$

which means the observer gain $H = P^{-1}Y$ is given by

$$H = \begin{bmatrix} 0.59 \\ -1.72 \cdot 10^{-4} \\ -0.020 \\ 0.040 \end{bmatrix} \quad (58)$$

and $Z_2 = 0.77$. The optimization yielded an upper bound of 2.84 on the $\mathscr{H}_2$ norm. At this point, the stabilizing gain H was used to form a left-coprime factorization as follows

$$\begin{bmatrix} \tilde{M}(\rho) & \tilde{N}(\rho) \end{bmatrix} = \left[\begin{array}{cccc|cc} 0.96 & 1.76 \cdot 10^3 & 0 & 0 & 0.59 & 1 \\ 0 & 0.48 & 0.0020 & 0 & -1.72 \cdot 10^{-4} & 0 \\ 0 & (3,2) & 0.99 & (3,4) & -0.020 & 0 \\ -0.0019 & 119.63 & 0 & 0.94 & 0.040 & 0.097 \\ \hline 0 & 2312.40 & 0 & 0 & 0.77 & 0 \end{array}\right], \quad (59)$$

where

$$(3,2) = -57.36 - 109.67\rho_1(k) + 89.58\rho_1(k)\rho_2(k) \quad (60)$$
$$(3,4) = -0.031 + 1.69\rho_1(k) - 1.38\rho_1(k)\rho_2(k). \quad (61)$$

The values were truncated to two significant figures for better visualization.

Next, the robust stabilization problem is solved by applying Theorem 5 to the system, described as a full information interconnection. The resulting matrices are

$$W = \begin{bmatrix} 163.19 & -3.12 \cdot 10^{-6} & 0.0018 & 0.021 \\ \star & 5.71 \cdot 10^{-10} & -6.00 \cdot 10^{-8} & -2.20 \cdot 10^{-7} \\ \star & \star & 1.68 \cdot 10^{-5} & 1.12 \cdot 10^{-4} \\ \star & \star & \star & 0.010 \end{bmatrix}, \quad (62)$$

$$Z = \begin{bmatrix} -0.73 & 2.88 \cdot 10^{-5} & -4.60 \cdot 10^{-4} & -0.12 \end{bmatrix}. \quad (63)$$

Thus, the state-feedback controller is given by

$$F = [0.042 \ \ 5267.10 \ \ 79.07 \ \ -9.78] \quad (64)$$

An upper bound on the induced-$\mathscr{L}_2$ norm is given by $\gamma = 3.15$, which means the robustness specification is met.

From the gains H and F, we can construct the controller in (17),

$$K_F(\rho) = \left[\begin{array}{cccc|c} 1.00 & 7.33 \cdot 10^3 & 79.07 & -9.78 & 0.59 \\ 0 & 0.48 & 0.0020 & 0 & -1.72 \cdot 10^{-4} \\ 0 & (3,2) & -1.00 & (3,4) & -0.020 \\ 0.0022 & 625.37 & 7.59 & 0.099 & 0.040 \\ \hline -0.042 & -5.27 \cdot 10^3 & -79.07 & 9.78 & 0 \end{array}\right], \quad (65)$$

where

$$(3,2) = -57.36 - 109.67\rho_1(k) + 89.58\rho_1(k)\rho_2(k) \quad (66)$$
$$(3,4) = -0.031 + 1.69\rho_1(k) - 1.38\rho_1(k)\rho_2(k). \quad (67)$$

Finally, the controller must be combined with the pre- and post-filters in (54) e (55), as explained in (27). Then, the final controller is ready for implementation.

Due the inherent time-variant nature of the system, traditional LTI concepts such as transfer functions and poles do not apply to problem at hand. However, as Apkarian et al. (1995) points out, LPV systems can also be interpreted as LTI systems with uncertainties. Using this notion, it we can compute the poles of the stabilized system in (59) and the final closed-loop system for different combinations of the scheduling parameters. Figure 3 shows that for a large set of parameters spanning the whole polytope, all poles lie in the unit circle for both systems.

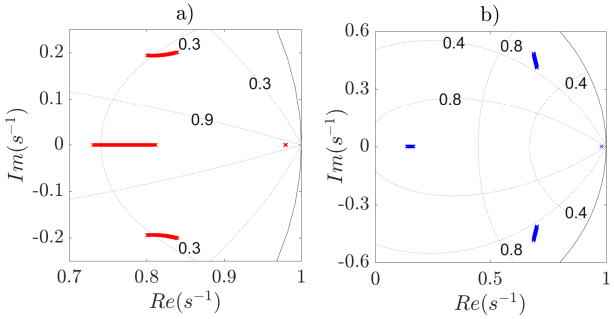

Figure 3. Stability assessment. a) pole locations for $A(\rho) + HC$. b) poles locations for $A(\rho) + HC + BF$.

5.2 Simulation

In order to assess the design specifications, the system was stabilized at position 9 mm and then subjected to

2 mm step inputs in both directions. As suggested by the manufacturer, a rate limiter of $5m/s$ rate limiter was used to slightly smooth the set-point changes. Figure 4 shows the ball position and applied voltage obtained in the simulation. The IAE value is 88.09, while the maximum overshoot is 5.83% and the settling time with 5% steady-state criterion is 420 ms. Figure 5 shows the coil current verified in the simulation.

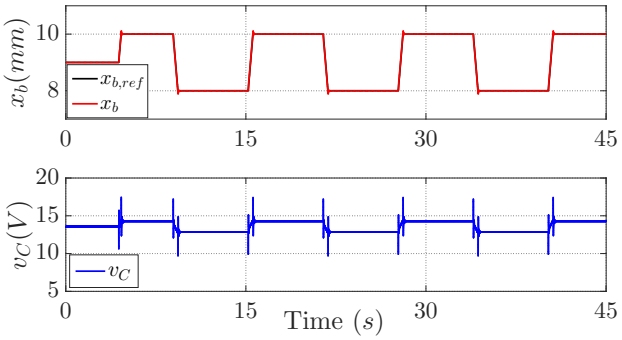

Figure 4. Simulation: ball position x_b and voltage v_C vs. time.

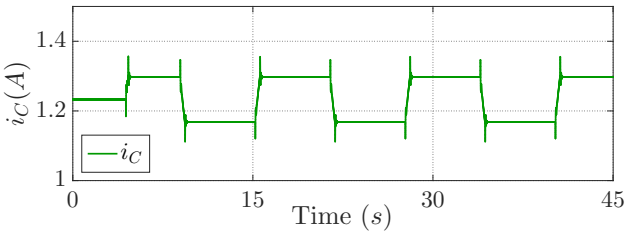

Figure 5. Simulation: coil current i_C vs. time.

The results at the simulation level were satisfactory, so the same controller gains were used to control the actual plant.

5.3 Experimental results

Figure 4 depicts the ball position and the voltage applied to the coil during the actual experiment. Naturally, the IAE value is much higher at 573.68. Part of this discrepancy is caused by sensor noise and unmodeled dynamics. Still, higher maximum overshoot at 11.75% and settling time at 490 ms also contribute to this increase.

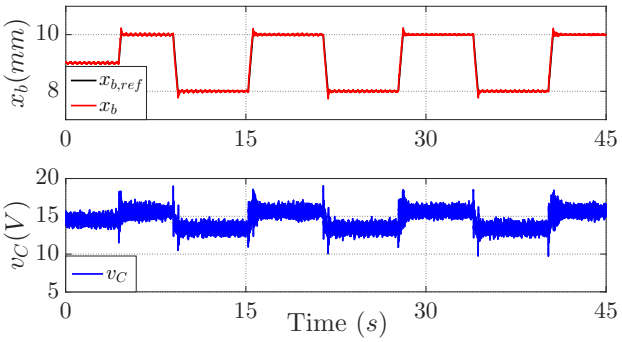

Figure 6. Experiment: ball position x_b and voltage v_C vs. time.

The coil current, which is a scheduling parameter, can be seen in Figure 7.

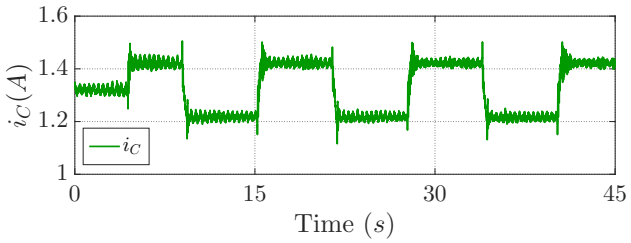

Figure 7. Experiment: coil current i_C vs. time.

Finally, Figure 8 shows the polytope as well as the scheduling parameters trajectories during the experiment. Notice that both varying parameters lie inside the polytope at all times.

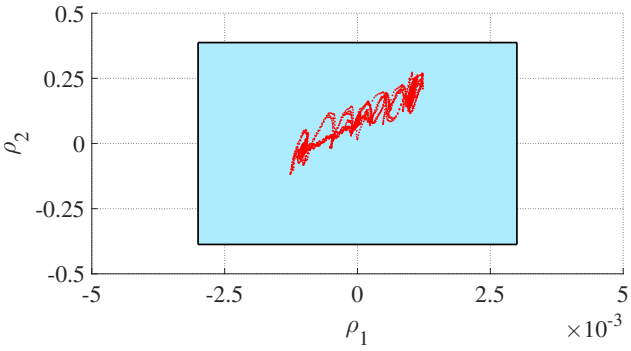

Figure 8. Experiment: parameter space and parameter trajectory.

As pointed out in Section 4, by fixating the varying parameters to be $\rho(k) = 0$ a reference LTI model at the operating point is recovered. Then, the synthesis used in this work should give a comparable result to the discrete-time $\mathscr{H}_\infty$ loop-shaping synthesis in Pereira et al. (2017b). This synthesis was also applied to the Maglev System. The graphs are omitted here for brevity, in favor of a numerical comparison.

Naturally, the upper bounds on the norm values for the LTI case are expected to be lower, since the polytope is degenerated to a point. That was indeed the case, with the $\mathscr{H}_2$ norm bounded by 2.61 and the $\mathscr{H}_\infty$ norm by 2.33. The parameter-varying entries in the LPV model feature a quadratic dependence on varying parameters, described by the polynomials in (53). These surfaces are rather flat within a certain range from the operating point, so the linear model is a relatively good approximation of the nonlinear dynamics. Still, the maximum overshoot is higher at 17.1%, while the settling time was similar at 500 ms.

6. CONCLUSION

This paper has shown the application of discrete-time $\mathscr{L}_2$ loop-shaping control to a Maglev system. The design is carried out in a simple and straightforward fashion, drawing intuition from classical control. Results were considered satisfactory both in terms of performance assessment and

robustness margins. Notwithstanding, quadratic stability imposes conservative bounds. Discrete-time static $\mathscr{L}_2$ lopshaping for LPV systems with bounded parameter variation remains an open problem. Hence, it is a nice idea for future works.

REFERENCES

Apkarian, P. (1997). On the discretization of lmi-synthesized linear parameter-varying controllers. *Automatica*, 33(4), 655–661.

Apkarian, P. and Gahinet, P. (1995). A convex characterization of parameter-dependent $\mathscr{H}_\infty$ controllers. *IEEE Transactions on Automatic Control*, 40, 853–864.

Apkarian, P., Gahinet, P., and Becker, G. (1995). Self-scheduled H_∞ control of linear parameter-varying systems: a design example. *Automatica*, 31, 1251–1261.

Balas, G. and Apkarian, P. (1992). Design of robust, time-varying controllers for missile autopilots. In *Proceedings 1st IEEE Conf. on Control Applications*.

Balini, H., Witte, J., and Scherer, C. (2012). Synthesis and implementation of gain-scheduling and LPV controllers for an AMB system. *Automatica*, 48, 521–527.

Barmish, B. (1985). Necessary and Sufficient Conditions for Quadratic Stabilizability of an Uncertain System. *Journal of Optimization Theory and Applications*, 46(4), 399–408.

Beck, C. and Doyle, J. (1993). Model reduction of behavioural systems. In *32nd Conference on Decision and Control*, 244, 3652–3657.

Becker, G. and Packard, A. (1994). Robust performance of linear parametrically varying systems using parametrically-dependent linear feedback. *System & Control Letters*, 23(3), 455–461.

Becker, G., Packard, A., Philbrick, D., and Balas, G. (1993). Control of parametrically-dependent linear systems. In *Proceedings of American Control Conf.* San Francisco.

Gahinet, P., Apkarian, P., and Chilali, M. (1996). Affine parameter-dependent Lyapunov functions and real parametric uncertainty. *IEEE Transactions on Automatic Control*, 41(3), 436–442. doi:10.1109/9.486646.

Gu, D.W., Petkov, P., and Konstantinov, M. (2002). Formulae for discrete H_∞ loop shaping design procedure controllers. *IFAC Proceedings Volumes*, 35(1), 109 – 113. doi:https://doi.org/10.3182/20020721-6-ES-1901.00353. 15th IFAC World Congress.

Gu, D., Petkov, P., and Konstantinov, M. (2013). *Robust control design with MATLAB*. Springer-Verlag, London.

Lescher, F., Zhao, J., and Borne, P. (2006). Switching lpv controllers for a variable speed pitch regulated wind turbine. In *IMACS Multiconference on Computational Engineering in Systems Applications*, 1334–1340.

Li, L. and Paganini, F. (2005). Structured coprime factor model reduction based on LMIs. *Automatica*, 41(1), 145–151.

Li, L. (2014). Coprime factor model reduction for discrete-time uncertain systems. *Systems & Control Letters*, 74, 108–114. doi:10.1016/J.SYSCONLE.2014.08.010.

Lovera, M., Novara, C., dos Santos, P., and Rivera, D. (2011). Guest editorial special issue on applied LPV modeling and identification. *IEEE Trans. Contr. Syst. Technol.*, 19(1), 1–4.

Lu, B., Buckner, G., and Tammi, K. (2008). Linear parameter-varying techniques for control of a magnetic bearing system. *Control Engineering Practice*, 16, 1161–1173.

McCloy, H., Dona, J., and Seron, M. (2018). Control of a Maglev System using the LPV framework: A tutorial from modelling to experimental implementation. *IFAC-PapersOnLine*, 51, 100–105.

McFarlane, D., Glover, K., and Vidyasagar, M. (1990). Reduced-order controller design using coprime factor model reduction. *IEEE Transactions on Automatic Control*, 35(3), 369–373. doi:10.1109/9.50362.

Packard, A. (1994). Gain scheduling via linear fractional transformations. *Systems & Control Letters*, 22(3), 79–92.

Pereira, R.L., Kienitz, K.H., and Guaracy, F.H.D. (2017a). Discrete-time static H_∞ loop shaping control for LPV systems. *25th Mediterranean Conference on Control and Automation (MED)*, 619–624. doi:10.1109/MED.2017.7984186.

Pereira, R.L., Kienitz, K.H., and Guaracy, F.H. (2017b). Discrete-time static H_∞ loop shaping control via LMIs. *Journal of the Franklin Institute*, 354(5), 2157–2166. doi:10.1016/J.JFRANKLIN.2017.01.009.

Prempain, E. (2004). Static h_∞ loop shaping control. In *UKACC International Conference on Control (CONTROL 2004)*, 244, 1334–1340.

Prempain, E. (2006). On Coprime factors for Parameter-Dependent Systems. *Proceedings of the 45th IEEE Conference on Decision and Control*, 5796–5800. doi:10.1109/CDC.2006.376773.

Prempain, E. and Postlethwaite, I. (2008). L_2 and H_2 performance analysis and gain-scheduling synthesis for parameter-dependent systems. *Automatica*, 44(8), 2081–2089. doi:10.1016/J.AUTOMATICA.2007.12.008.

Quanser, Inc. (2012). Instructor workbook: Magnetic levitation experiment for matlab/simulink users.

Sefton, J. and Glover, K. (1990). Pole/zero cancellations in the general hâˆž problem with reference to a two block design. *Systems & Control Letters*, 14(4), 295 – 306. doi:https://doi.org/10.1016/0167-6911(90)90050-5.

Shahruz, S., Behtash, S., and Seron, M. (1992). Design of controllers for linear parameter varying systems by the gain scheduling technique. *J. Math. Anal. Appl.*, 168, 195–217.

Shamma, J. (1988). *Analysis and Design of Gain Scheduled Control Systems*. Ph.D. thesis, MIT, Cambridge, USA. Supervisor: Michael Athans.

Shamma, J. and Athans, M. (1990). Analysis of Gain Scheduled Control for Nonlinear Plants. *IEEE Transactions on Automatic Control*, 35, 898–907.

Tonoli, A., Bonfitto, A., Silvagni, M., and Suarez, L.D. (2012). Rotors on active magnetic bearings: Modeling and control techniques. In *Advances in Vibration Engineering and Structural Dynamics*, 1–3. InTech.

Toth, R. (2010). *Modeling and identification of linear parameter-varying systems*. Lecture notes in control and information sciences. Springer, Germany.

Wang, F. and Balakrishnan, V. (2002). Improved stability analysis and gain-scheduled controller synthesis for parameter-dependent systems. *IEEE Transactions on Automatic Control*, 47(5), 720–734.

Whidborne, J., Postlethwaite, I., and Gu, D. (1994). Robust Controller Design Using H_∞ Loop-Shaping and the Method of Inequalities. *IEEE Trans. Contr. Syst. Technol.*, 2(4), 455–461.

Wu, F. (1995). *Control of Linear Parameter Varying Systems*. Ph.D. thesis, University of California at Berkeley, Berkeley, USA.